

Echo-planar rotating-frame imaging

F. Casanova,* H. Robert,¹ J. Perlo, and D. Pusiol

Facultad de Matemática, Astronomía Física, Universidad Nacional de Córdoba, Astronomía y Física, Ciudad Universitaria, Córdoba 5000, Argentina

Received 25 October 2002; revised 17 March 2003

Abstract

A new rotating-frame imaging method that produces a complete cross section of an object in a single experiment is reported. The echo planar rotating frame imaging (EPROFI) technique uses two perpendicular RF gradients for two-dimensional spatial encoding and fully exploits the formation of rotary echoes for fast sampling of spatial frequencies. The acquisition scheme yields the Fourier transform of the spin distribution on Cartesian coordinates for straightforward image reconstruction. Implementation of the technique on a low-field portable NMR probe is described and results are presented for test objects with different geometries.

© 2003 Elsevier Science (USA). All rights reserved.

Keywords: Magnetic resonance imaging; Rotating-frame imaging; Echo planar imaging; RF gradients; Spatial encoding

1. Introduction

Spatial localization techniques based on radiofrequency (RF) B_1 -field gradients present some advantages over the conventional encoding methods that use B_0 gradients, in particular for small volume imaging applications [1–11]. Encoding techniques based on B_1 gradients have the potential to alleviate distortion effects due to magnetic susceptibility variations and B_0 inhomogeneities across the object, and allow the application of strong encoding gradients with short rise and fall times.

In the presence of a RF field gradient, nuclear spins immersed in a strong static magnetic field nutate at a rate defined by the local value of the excitation field. The flip angle of the spin magnetization, $\theta = \gamma B_1(\mathbf{r})t_1$, is defined by the local RF field strength $B_1(\mathbf{r})$, where \mathbf{r} represents the spatial spin coordinates, and the total duration t_1 of the excitation pulse. Sampling of the spatially variable nutation frequency $\omega_1(\mathbf{r}) = \gamma B_1(\mathbf{r})$ is then possible by measuring FID's parameters for various excitation pulse widths t_1 or for incremental RF amplitudes. Depending on the encoding sequence, spa-

tial information becomes encoded in the amplitude or phase of the spin magnetization. A linear dependence of B_1 magnitude with spatial coordinates is desirable for straightforward image reconstruction. The original NMR rotating-frame technique suggested by Hoult [1] allows one to image a spin density distribution along the axis defined by the RF gradient. In the absence of static read-out gradient the technique provides a spatially resolved spectroscopy method, which can be used to measure spatial distribution of physical parameters in the object. Rotating-frame NQR Imaging (ρ NQRI) exploits this advantage of the technique for spatial mapping of physical parameters such as temperature and strain [12,13].

With the original rotating-frame imaging technique [1] each encoding step is preceded by a waiting time longer than the spin-lattice relaxation parameter. Localization along multiple dimensions is therefore a very time consuming experiment. It has been demonstrated that a considerable reduction in data collection time is possible by disregarding spectroscopic resolution. A one-fold reduction in the dimensionality of the experiment can be achieved by sampling the magnetization in the course of nutation driven by RF excitation [4,5,8,9]. High RF power is needed to achieve high spatial resolution and the well-known leakage problems associated with simultaneous excitation and detection preclude the application of a CW technique. The rapid rotating-

* Corresponding author. Fax: +49-241-8022185.

E-mail address: fcasanova@mc.rwth-aachen.de (F. Casanova).

¹ Present address: Quantum Magnetics, 7740 Kenamar Crt, San Diego, CA 92121, USA.

frame technique uses a train of strong RF pulses for stroboscopic acquisition of the nuclear magnetization and achieves one-dimensional localization in a single experiment. The pulse sequence consists of a train of short RF pulses with a constant gradient and separated by short intervals τ of free evolution for signal sampling. The train of N *encoding* and *read* pulses for the rapid rotating-frame technique is here denoted as $(\theta_p - \tau)_N$, where $\theta_p = \omega_1(p)\Delta t_p$ is the flip angle induced by a RF pulse of strength B_1 and duration Δt_p , applied with a constant gradient along the p -axis of the laboratory frame ($p = x, y, z$). The sampling interval Δt_p determines the field of view and it is adapted to the size of the object to avoid aliasing of spatial frequencies. The acquisition window τ is much shorter than the lifetime of the FID T_2^* , so that the nutation angles of the magnetization accumulate and the effective tilt angle after N pulses is $\Theta_p = N \times \theta_p$. Sampling of the spatial frequencies occurs by accumulating flip angles that modulates the FID's amplitude. The effects of relaxation during the pulse train have been addressed by Maffei et al. [8]. Recently, we demonstrated a phase-encoded variant of the technique for improved sensitivity [14].

Two-dimensional images using the 1D rapid-rotating frame technique were first obtained simply by recording a set of 1D projections for different orientations of the sample with respect to the RF gradient direction [8]. A map of the spin density in the x - y plane was then reconstructed on a Cartesian grid by a standard filtered back-projection algorithm. We have reported [15] that 2D images of quadrupolar nuclei can be obtained by an encoding procedure based on the irradiation of the object by a pulse sequence with orthogonal RF gradients. A preparatory RF pulse with gradient $g_1(x)$ in the x direction is first applied and it is followed by a 1D rapid rotating-frame irradiation sequence with the read gradient $g_1(y)$ along the y -axis. The multiple-pulse sequence is

$$m\theta_{x,\phi} - T - (\theta_{y,\phi'} - \tau)_N,$$

where $m\theta_{x,\phi}$ denotes a pulse of length $m\Delta t_x$ and ϕ is the phase in the rotating frame. If the interval T is much shorter than T_2 , the preparatory pulse can be applied in such a way that the spatial information becomes encoded either in the phase or amplitude of the signal. When the time interval T is much longer than the spin-spin relaxation parameter, the relative phase between the preparatory pulse and the read pulses is irrelevant and the spatial information on the x -axis results encoded in the amplitude of the pseudo-FID. The irradiation sequence is repeated for a set of M durations of the preparatory pulse, $m = 1, \dots, M$. This method does not involve rotation of the object and the 2D spin density distribution $\rho(x, y)$ is mapped directly on Cartesian coordinates.

In the above-mentioned 2D encoding techniques each irradiation sequence is followed by a waiting time T_R

longer than T_1 , which enables the spin system to return to thermal equilibrium before the next encoding step, sample rotation or preparatory pulse increment, proceeds. Therefore, a complete 2D experiment demands a rather long measuring time of about $M \times T_R$, where M is either the number of increments in the preparatory pulse or rotation steps of the object.

In addition to spatial resolution, the speed at which a complete picture can be produced is an important criterion for the observation of a system evolving on a very short time scale. The aim of this work is to demonstrate that one can devise a procedure similar to echo-planar imaging (EPI) [16] based on RF gradients. The goal of our rotating-frame imaging procedure is to render a complete cross-sectional spin image in a single pulse train. The basic idea to speed up data acquisition relies on the fact that in spin systems with long enough T_2 , the magnetization dispersed in the presence of a non-uniform RF field can be refocused as a *rotary echo* [17]. Let's consider a train of RF gradient pulses applied for 1D encoding purposes to the nuclear magnetization in its thermal equilibrium state. Because of the presence of an inhomogeneous B_1 field the nuclear magnetization vectors at different parts of the sample fan out in the plane perpendicular to the B_1 field in the absence of any off-resonance effects. After applying N pulses of duration Δt_x , a 180° phase shift of the RF field is performed; so that B_1 is suddenly reversed in the rotating frame. Then, a train of pulses with inverted phase will refocus the magnetization vectors after N pulses along the z -axis producing a *rotary echo*. Subsequent phase inversions of B_1 at $3N\Delta t_x$, $5N\Delta t_x$, etc produces echoes at $4N\Delta t_x$, $6N\Delta t_x$, etc. Alternatively, the magnetization can be taken back to the z -axis by a long 180° out-of-phase RF pulse of duration $\Theta_x = N\theta_x$.

The fast 2D NMR imaging technique with B_1 gradient recently proposed by Raulet et al. [18] combines RF irradiation of the sample by the pulse sequence

$$[(\theta_{x,0^\circ} - \tau)_N - N\theta_{x,180^\circ}]_M$$

with continuous rotation of the object for fast sampling of 2D spatial information. After a series of dummy defocusing-refocusing processes a steady-state is reached and collection of a set of 1D profiles proceeds. A two-dimensional image is then reconstructed by filtered back-projection. By this procedure they managed to lower the acquisition time with liquid-like samples from several minutes down to a few seconds.

In this paper, a new planar rotating-frame imaging method is proposed that fully exploits the formation of rotary-spin echoes. The echo-planar rotating-frame imaging (EPROFI) technique employs two perpendicular RF gradients and continuous defocusing-refocusing of the magnetization for rapid sampling of the \mathbf{k} -space. As in the modified echo-planar acquisition scheme, known as BEST and MBEST [19], the scanning pattern gives

the Fourier transform of the spin density function $\rho(\mathbf{k})$ on a rectangular grid. Reconstruction of $\rho(x, y)$ is easily accomplished by an ordinary 2D discrete Fourier transformation. In the following sections, we describe the implementation of the technique and report results using a low-field portable NMR system.

2. The EPROFI technique

The rotating-frame encoding pulse sequence to produce a cross-sectional image of the spin density in a single scan is depicted in Fig. 1. A series of rotary- or pseudo-echoes is formed by the pulse sequence

$$[(\theta_{x,0^\circ} - \tau)_N - (\theta_{x,180^\circ} - \tau)_N]_M$$

applied with the *read* RF gradient $g_1(x)$ (Fig. 1a). Each rotary echo samples the x -dimension of the \mathbf{k} -space from zero to $+k_{x,\max}$ and back to zero, where $k_{x,\max} = \gamma|g_1(x)|N\Delta t_x$. Spatial localization in the second dimension is achieved by including in the pulse train of $g_1(x)$ pulses a second RF field B_2 with pulses of length Δt_y , applied with the second gradient $g_1(y)$ along the y -axis (Fig. 1b). The complete pulse sequence for fast 2D imaging with RF gradients is

$$[(\theta_{x,0^\circ} - \tau)_N - (\theta_{x,180^\circ} - \tau)_N - \theta_{y,90^\circ}]_M.$$

It can easily be seen that the nutation angles θ_y are not refocused by the orthogonal $g_1(x)$ pulses and they accumulate as the encoding process advances in complete analogy to the phase accumulation introduced by the blipped pulses in the EPI sequence [19] (Fig. 1c).

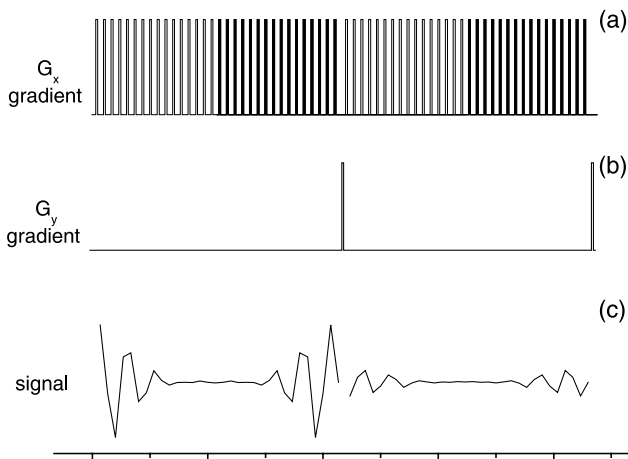


Fig. 1. Pulse sequence for the EPROFI technique: RF field gradients along the x and y directions, $g_1(x)$ and $g_1(y)$, are applied as hard pulses separated by short acquisition windows. (a) Trains of $g_1(x)$ pulses with alternating phase in the rotating frame between zero (white pulses) and 180° (black pulses) to refocus the spin magnetization as a series of pseudo-echoes. (b) RF pulses with a gradient along y are applied after each rotary echo, thus modulating the amplitude of the pseudo-echoes according to the position of the spins along the y coordinate. (c) The first two pseudo-echoes constructed by acquiring a single data point in each interval between $g_1(x)$ pulses are shown.

Therefore, after the m th encoding pulse, the nutated angle θ_y is proportional to $k_y y$, where $k_y = \gamma g_1(y) m \Delta t_y$, and the y -dimension of the \mathbf{k} -space is sampled from the center to $k_{y,\max} = \gamma g_1(y) M \Delta t_y$. The two perpendicular RF gradients needed for the implementation of this pulse sequence were delivered by two independent RF surface coils whose geometries are described in the next section. These coils are able to produce field gradients that can be considered nearly constant along the x and y directions plane. Assuming constant and orthogonal RF gradients over the volume of the sample, the calculation of the evolution of the nuclear magnetization is straightforward and the detected in-phase component of the spin response is

$$S(k_x, k_y) = \int_{-\infty}^{+\infty} dy \int_{-\infty}^{+\infty} dx B_1(x) \rho(x, y) \sin(k_x x) \times \cos(k_y y). \quad (1)$$

We assumed the surface coil delivering the $g_1(x)$ gradient is also used for signal detection, and the spatial dependence of the receiver coil's sensitivity is included in Eq. (1) according to the well-known reciprocity principle [20]. This distortion is easily removed from the reconstructed image by weighting the profiles along y -axis with the inverse of the $B_1(x)$'s profile [9].

This method samples only one quadrant, $x \geq 0$ and $y \geq 0$, of the \mathbf{k} -space and the final image is reconstructed by using a 2D-FT. In order to achieve higher spatial resolution it is desirable to obtain the image in a 2D pure-absorption spectrum. One of the advantages of the encoding scheme described above is that the signal is amplitude modulated in both dimensions. Therefore, a two-dimensional spectrum in pure absorption mode can be obtained by using a real FT with respect to t_x and a complex FT along t_y [21]. The sine transform of the sine amplitude-modulated signal leads to a real 2D spectrum fully symmetric along the first spatial dimension x . After performing a complex FFT along the t_y dimension the spectrum is also symmetric on the second dimension y . The image is then obtained in the first quadrant of the real spectrum. It should be pointed out that several variants of the 2D encoding pulse sequence can be devised for full \mathbf{k} -space sampling or phase encoding along y -axis. For the sake of simplicity and convenience we restrict ourselves in the next sections to discuss the 2D amplitude-modulated version of the technique.

No attempt has been made in this work to implement a slice selection procedure to control the slice thickness or third dimension z . In principle, the slice thickness can be limited over the plane defined by the encoding RF gradients by implementing a suitable technique based on RF gradients [6,8] or by conventional procedures using pulsed DC magnetic field gradients [10,19]. In our experiments the cross section was defined simply by physically limiting the sample's thickness to about 1 mm.

Maffei et al. [8] have shown that during the application of the RF pulses the nuclear magnetization in liquid-like samples decays according to the relaxation time $T_{12}^{-1} = (T_1^{-1} + T_2^{-1})/2$, while during the acquisition windows the decay is imposed by T_2 for the in-plane magnetization and by T_1 for the longitudinal component. Therefore, the amplitude of the rotary echoes generated by the pulse sequence of Fig. 1a decays with a time constant T_{eff} that is approximately given by T_{12} . The maximum number of sampling points on a square grid ($N = M$) in the \mathbf{k} -space that can be collected with the EPROFI encoding technique is roughly given by $N^2 = T_{12}/(\Delta t_x + \tau)$.

3. Experiments and results

The experiments were carried out on a home-built spectrometer equipped with a dedicated probe. The RF probe designed for these experiments includes two perpendicular surface coils to deliver approximately orthogonal RF gradients. A two-turn solenoid of 18 mm diameter generates the $g_1(x)$ gradient along the x -axis and collects the NMR signal. A rectangular coil, 30 mm \times 18 mm, produces the second RF gradient $g_1(y)$ along the y -axis [15]. A major difficulty in this setup is the adjustment of the relative position of the coils in order to obtain the optimum gradient uniformity and maximum electric decoupling. More sophisticated schemes can be used to achieve higher decoupling. After minimizing the coupling, the RF probe was tuned at 13.74 MHz that corresponds to the proton resonance frequency as defined by our permanent magnet.

A Kalmus LP1000 power amplifier drives the rectangular coil, whereas a 300 W Motorola Mod. 827 amplifier is used for the circular coil. The output powers of the RF amplifiers were adjusted to assure similar RF gradient strengths, of the order of 14 G/cm, in both spatial directions. Analog phase-shifters were inserted in each transmitter path to adjust carefully the phase of both channels relative to the reference. Appropriate phase cycling was provided by a computer-controlled PTS 310 frequency synthesizer.

The static magnetic field is provided by permanent SmCo magnets mounted on an iron yoke with an air gap of 20 mm. The magnets are cylinders of 7.5 cm diameter and 2.5 cm thickness. This geometry provides a magnetic field strength of 0.32 T. Field inhomogeneities in this design determines a time-decay constant for the FID of about 1.5 ms at the center of the gap.

The EPROFI pulse sequence was implemented with a train composed of 32 sets of 32 read pulses in each set. The $g_1(x)$ pulses were 7 μ s long, separated by acquisition windows of 30 μ s. For spatial encoding along the second dimension, $g_1(y)$ pulses of 7 μ s duration were applied as described in Eq. (1). With this encoding scheme, a

32×32 data matrix was acquired in about 75 ms. The raw data set was zero-filled to 512×512 and a 2D FFT yielded a cross section of the sample in the real part of the 2D spectrum. Under the assumption of constant RF gradients over the object a linear correction was implemented to compensate for the spatial sensitivity dependence of the receiver coil on the x direction.

The low sensitivity of our system, resulting mainly from the very low polarization field, precluded the acquisition of a full 2D image in a single scan. About 200 averages per experiment were required to increase the SNR. Obviously, increasing the B_0 strength will result in improved sensitivity, longer T_{eff} , and shorter dead times leading to the possibility of recording a 2D image in a single pulse train.

In order to evaluate the linearity and orthogonality of the radiofrequency gradients, we performed numerical calculations of the spatial distribution of the magnetic field produced by the gradient coils, taking into account only the field's components transverse to the external static magnetic field. These results determined the maximum size of the object to be placed so that distortions over each dimension would be less than the pixel resolution.

The first test employed an object made of gelatine to avoid meniscus and wetting problems that appear with liquids on the walls of the sample holder, thus providing a 1 mm homogeneous slice. The relaxation times T_1 and T_2 were measured in independent experiments and the values are 1.2 s and 130 ms, respectively. Fig. 2a shows the first 16 rotary echoes obtained without the application of the RF pulses along the second dimension; thus making possible to observe the decay of the echo train dictated by T_2 in agreement with the value of T_{eff} proposed by Maffei et al. [8]. The modulation in the echo amplitude when introducing the $g_1(y)$ RF pulses is apparent in Fig. 2b. The cross-section of the phantom in Fig. 3a and the image obtained after averaging 200 scans and reconstructed by 2D Fourier transformation is shown in Fig. 3b. Since the final image reproduces a fair structure of the object without appreciable distortions, we conclude that the assumption of constant gradients over the volume of the object is acceptable. Testing with larger objects yielded distorted images due to departure of the RF fields from linearity over the volume of the sample.

Further testing of the technique were carried out on a 1 mm height and 3 mm diameter onion's stem. The relaxation parameter values are $T_1 = 1$ s and $T_2 = 155$ ms; therefore, the time decay parameter of the echo train is roughly given by T_2 . The time-domain data set was acquired in about 75 ms, which makes relaxation effects almost negligible during acquisition. A picture of the onion's slice is shown in Fig. 4a and the final image obtained with the EPROFI method is presented in Fig. 4b. The image in Fig. 4b was reconstructed under the

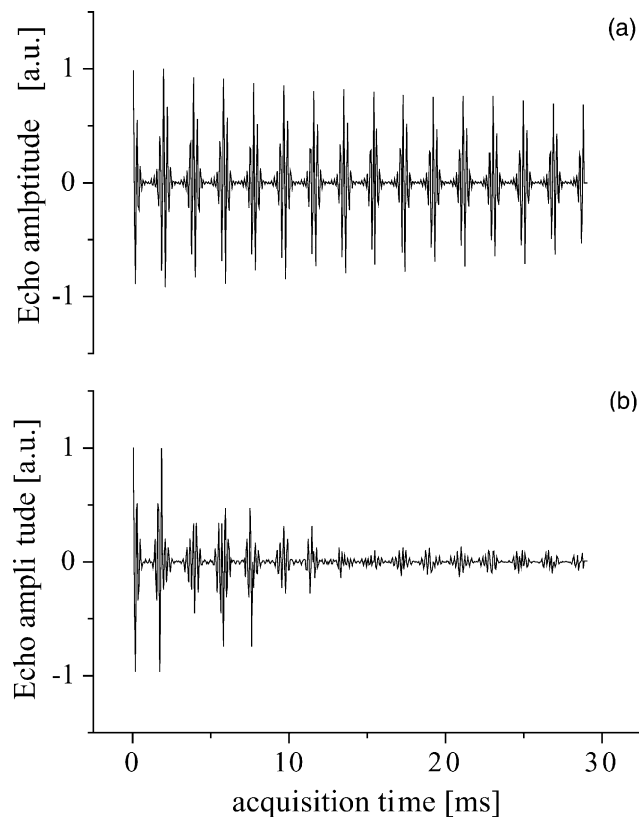


Fig. 2. (a) Rotary echoes formed by applying the sequence shown in Fig. 1a. The decay observed in the envelope of the echoes is in agreement with the value calculated from the T_1 and T_2 values according to Eq. (1). (b) Train of rotary echoes modulated in amplitude by applying $g_1(y)$ pulses as shown in Fig. 1b. The pseudo-echo train contains the information necessary to reconstruct a cross-section of the object on the x - y plane.

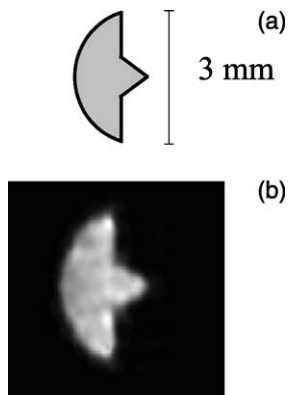


Fig. 3. (a) Geometry of the test object used for testing the EPROFI technique. A 3 mm-diameter container made of Teflon was filled with gelatin. Gelatin was chosen as the proton source because it provides a uniform slice and it has convenient relaxation parameters for evaluating our encoding method. The object is uniform along the longitudinal axis and no slice selection procedure was applied. (b) Two-dimensional NMR image constructed from data acquired using the EPROFI technique shown in Fig. 1. A total of 200 scans were averaged to increase the SNR using a recycling delay of 2 s. No spatial distortions are apparent in the image because of the small diameter of the object compared to the overall dimension of the coils.

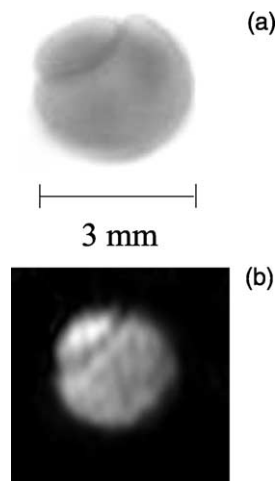


Fig. 4. (a) Picture of a onion's stem slice, 1 mm height and 3 mm diameter, used for further evaluation of the fast 2D encoding technique. (b) Two-dimensional spatial distribution reconstructed by 2D-FFT from data gathered with the EPROFI method. Parameters of the pulse sequence were identical to the values used for the experiment shown in Fig. 3. The total number of scans was 400.

assumption of constant RF gradients; i.e., no correction to spatial coordinates were applied to compensate for non-linearity of the RF gradients.

4. Conclusions

A number of interesting applications of NMR imaging by RF field gradients, such as observation of solvent penetration in polymeric materials [22], the study of human organs [23], mapping of current density [24], have been reported. In some applications, the quasi-immunity of rotating-frame encoding techniques to magnetic susceptibility distortions was exploited to achieve good-quality images in spite of broad NMR lines [25], and it has been demonstrated that the method affords microscopic spatial resolution. We believe that rendering of 2D spin distributions by the EPROFI method is a promising technique for studying systems in which the measuring time becomes important or in situations where motion is present.

Besides the potential for high-speed 2D imaging, the advantages of the described encoding technique in the rotating frame compared to the method presented in [18] are that rotation of the object is not required and the spin density function is sampled directly on a cartesian grid.

It would be advantageous to improve the design of our RF gradient coils for maximum filling factors and more uniform RF gradients over the sample's volume. Higher B_0 fields are obviously desirable not only for higher SNR but also for shorter dead times and slower relaxation during the pulse train resulting in larger number of sampling points per scan.

Acknowledgments

The authors thank the National and Provincial Research Councils (CONICET and CONICOR). F.C. and J.P. thank CONICET for Research Fellowships.

References

- [1] D.I. Hoult, J. Magn. Reson. 33 (1979) 183.
- [2] D.I. Hoult, J. Magn. Reson. 38 (1980) 369.
- [3] M. Nuss, E.T. Olejniczak, J. Magn. Reson. 69 (1986) 542.
- [4] K.R. Metz, J.P. Boehmer, Magn. Reson. Imag. 6 (1) (1988) 53.
- [5] D. Boudot, D. Canet, J. Brondeau, J.C. Boubel, J. Magn. Reson. 83 (1989) 428.
- [6] D. Boudot, D. Canet, J. Brondeau, J. Magn. Reson. 87 (1990) 385.
- [7] D. Boudot, F. Montigny, K. Elbayed, P. Mutzenhardt, B. Diter, J. Brondeau, D. Canet, J. Magn. Reson. 92 (1991) 605.
- [8] P. Maffei, P. Mutzenhardt, A. Retournard, B. Diter, R. Raulet, J. Brondeau, D. Canet, J. Magn. Reson. A 107 (1994) 40.
- [9] K.R. Metz, J.P. Boehmer, J.L. Bowers, J.R. Moore, J. Magn. Reson. B 103 (1994) 152.
- [10] J.L. Bowers, P.M. Macdonald, K.R. Metz, J. Magn. Reson. B 106 (1995) 72.
- [11] F. Humbert, B. Diter, D. Canet, J. Magn. Reson. A 123 (1996) 242.
- [12] E. Rommel, D. Pusiol, P. Nickel, R. Kimmich, Meas. Sci. Technol. 2 (1991) 866.
- [13] P. Nickel, H. Robert, R. Kimmich, D. Pusiol, J. Magn. Reson. A 111 (1994) 191.
- [14] F. Casanova, H. Robert, D. Pusiol, J. Magn. Reson. 141 (1999) 62.
- [15] H. Robert, D. Pusiol, J. Magn. Reson. 127 (1997) 109.
- [16] P. Mansfield, J. Phys. C 10 (1977) L55.
- [17] L. Solomon, Phys. Rev. 2 (7) (1959) 301.
- [18] R. Raulet, D. Grandclaude, F. Humbert, D. Canet, J. Magn. Reson. 124 (1997) 259.
- [19] P.T. Callaghan, Principles of Nuclear Magnetic Resonance Microscopy, Clarendon Press, Oxford, 1991.
- [20] D.I. Hoult, R.E. Richards, J. Magn. Reson. 24 (1976) 71.
- [21] R.R. Ernst, G. Bodenhausen, A. Wokaun, Principles of Nuclear Magnetic Resonance in One and Two Dimensions, Clarendon Press, Oxford, 1987.
- [22] P. Maffei, L. Kiene, D. Canet, Macromolecules 25 (1992) 7114–7118.
- [23] M. Blackledge, P. Styles, G. Radda, J. Magn. Reson. 71 (1987) 246–258.
- [24] G.C. Scott et al., Magn. Reson. Med. 33 (3) (1995) 355.
- [25] R. Raulet, J.M. Escanye, F. Humbert, D. Canet, J. Magn. Reson. A 119 (1996) 111–114.